Strange vector form factors of the nucleon

Hilmar Forkel,* Marina Nielsen,† Xuemin Jin, and Thomas D. Cohen
Department of Physics and Center for Theoretical Physics, University of Maryland, College Park, Maryland 20742
(Received 8 April 1994)

A model combining vector meson dominance, ω-ϕ mixing, and a kaon cloud contribution is used to estimate the strangeness vector form factors of the nucleon in the momentum range of the planned measurements at MIT-Bates and CEBAF. We compare our results with some other theoretical estimates and discuss the nucleon strangeness radius in models based on dynamically dressed, extended constituent quarks. For a quantitative estimate in the latter framework we use the Nambu–Jona-Lasinio model.

PACS number(s): 14.20.Dh, 12.40.Vv, 12.15.Mn, 12.39.Ki

I. INTRODUCTION

Strangely, not all static low-energy properties of the nucleon are yet measured. In particular, practically no experimental information exists on the nucleon form factors of the strange-quark vector current, the subject of our paper. One might ask why these observables have so far escaped experimental scrutiny. Certainly they are not easy to measure, requiring high-statistics neutral current experiments at the limits of present capabilities, but perhaps more importantly they were widely expected to be zero or at least small.

In the absence of direct insight from QCD at low energies, these expectations had been guided by hadron models, and most prominently by the nonrelativistic quark model (NRQM) [1]. The latter gained particular credibility by describing the low-lying meson and baryon spectra better than other, and often more complex, hadron models. However, this model is based either on the complete neglect or at least on a drastic simplification of relativistic effects, which seems hard to justify in the light quark sector.

This limited treatment does of course not only affect the valence quarks. More importantly in our context, it excludes vacuum fluctuations and, in particular, the existence of virtual quark-antiquark pairs in the hadron wave functions. The nucleon, for example, is described as consisting solely of up and down constituent quarks, and the NRQM thus predicts the absence of any strangeness distribution.[1]

It therefore came as a surprise to many when deep inelastic μ-p scattering data from the European Muon Collaboration (EMC) [2] indicated a rather large strange-quark contribution to the singlet axial current of the nucleon. The EMC measured the polarized proton structure function $g_1^p(x)$ in a large range of the Bjorken variable, $x \in [0.01, 0.7]$ [2,3] and found, after Regge extrapolation to $x = 0$ and combination with earlier SLAC data,

$$\int_0^1 dx\, g_1^p(x) = 0.126 \pm 0.010\,(\text{stat}) \pm 0.015\,(\text{syst})\,, \quad (1.1)$$

at $Q^2 = 10\,\text{GeV}^2/c^2$. Ellis' and Jaffe's prediction [4], which neglected strange-quark contributions, was significantly larger: 0.175 ± 0.018. From the above data, however, one extracts a nonvanishing strange-quark contribution $\Delta s = -0.16 \pm 0.008$ to the proton spin or, equivalently, via the Bjorken sum rule, a substantial strangeness contribution to the proton matrix element of the isoscalar axial-vector current.

The low-energy elastic ν-p scattering experiment E734 at Brookhaven [5] complemented the EMC data by measuring the same matrix element at smaller momenta ($0.4\,\text{GeV}^2 < Q^2 < 1.1\,\text{GeV}^2$). The results of this experiment also contain information on the strange vector form factors and will therefore be discussed in more detail later, in Sec. II B. The extracted axial-vector current form factors are consistent with the muon scattering data from the EMC [6].

The scalar channel provides additional, although indirect, experimental evidence for a significant strangeness content of the nucleon [7–10]. It stems from the nucleon sigma term, $\Sigma_{\pi N}$, which can be extracted from pion-nucleon scattering data. Defining the ratio R_s as

$$R_s = \frac{\langle p|\bar{s}s|p\rangle}{\langle p|\bar{u}u + \bar{d}d + \bar{s}s|p\rangle}\,, \quad (1.2)$$

(u, d, and s are the up, down, and strange quark fields, and $|p\rangle$ denotes the nucleon state) one finds $R_s \simeq 0.1 - 0.2$. Again, the resulting $\langle p|\bar{s}s|p\rangle$ matrix element is surprisingly large, of up to half the magnitude of the corresponding up-quark matrix element. This implies that the nucleon mass would be reduced by $\approx 300\,\text{MeV}$ in a world with massless strange quarks. The analysis leading to the quoted range of R_s values is, however, not

*Present address: European Centre for Theoretical Studies in Nuclear Physics and Related Areas, Villa Tambosi, Strada delle Tabarelle 286, I-38050 Villazzano, Italy.
†Permanent address: Instituto de Física, Universidade de São Paulo, 01498 SP, Brazil.

[1] In some generalized constituent quark models, the quarks have an extended structure which can contain strangeness (see Sec. III E).

uncontroversial, and smaller values have been suggested [11].

In any case, there is evidence that strange quarks play a more significant role in the nucleon than the quark model suggests. One direction for the further exploration of this intriguing issue is to study the nucleon matrix elements of strange-quark operators in other channels. Since the electroweak neutral currents provide us with experimental probes in the vector channel, the strange vector current has recently received considerable attention. In particular, a number of devoted experiments at MIT-Bates [12] and CEBAF [13–15] (see Sec. II B) will measure part of the corresponding form factors at low momenta.

In this situation it would clearly be desirable to have reliable theoretical predictions for these form factors. Unfortunately, the present status of our theoretical understanding is qualitative at best. A phenomenological estimate and some model calculations have been performed, but all results have large theoretical uncertainties and are partially inconsistent with each other.

Since the sea quark distribution in hadrons arises from a subtle interplay of quantum effects in QCD, their reproduction in hadron models is much more challenging than the calculation of the standard static observables. Lattice calculations of strange-quark distributions have not yet been performed since the disconnected quark loops increase the computational demands of form factor calculations substantially.

The particular value of the strange-quark mass, which is neither light nor heavy compared to the QCD scale Λ, additionally complicates the theoretical situation. In contrast to the light up and down quarks, the effects of the heavier strange quark are much harder to approach from the chiral limit, i.e., by an expansion in the quark mass. On the other hand, the strange quark is too light for the methods of the heavy-quark sector, e.g., the nonrelativistic approximation or the heavy-quark symmetry, to work.

The purpose of this paper is to assess the present theoretical status by discussing some of the proposed models, and to extend our previous estimate of the nucleon strangeness radius in a vector dominance model to the calculation of the strangeness vector form factors in the momentum region of interest for the planned experiments.

In Sec. II we will set up our notation, give the basic definitions and discuss the presently available and soon to be expected experimental information. Section III contains a review of some theoretical estimates for the strangeness radius and magnetic moment, including the pole fit of Jaffe [16], a Skyrme model calculation [17], the kaon cloud model estimate [18], and our own estimate based on vector meson dominance and ω-ϕ mixing [19]. We conclude this section with a new calculation in the framework of extended constituent quark models, where the light quarks are dressed with a quark-antiquark cloud and carry strangeness. The fourth section describes the calculation of the strange vector form factors in our model, discusses our results, and compares them to the pole fit estimate and the sometimes used dipole form. In Sec. V we summarize the paper and present our conclusions.

II. BASIC CONCEPTS AND EXPERIMENTAL STATUS

In order to quantify the concept of the nucleon's strangeness distributions in the language of QCD, one considers nucleon matrix elements of the form

$$\langle p|\,\bar{s}\,\Gamma s\,|p\rangle, \tag{2.1}$$

where Γ stands for a Dirac matrix, which selects the space-time quantum numbers of the matrix element. These matrix elements are, in general, scale dependent. As indicated in the Introduction, we will discuss in particular the matrix element of the strange vector current (i.e., $\Gamma = \gamma_\mu$), which, due to strangeness conservation, is independent of the subtraction point of the current operator.

A. Basic definitions

Most of the theoretical work has so far focused on the lowest nonvanishing radial moments of the strangeness spin and charge distributions. These are the strangeness magnetic moment μ_s, defined as the z component of

$$\boldsymbol{\mu}_s = \frac{1}{2}\int d^3r\,\langle p|\mathbf{r}\times\bar{s}\boldsymbol{\gamma}s|p\rangle, \tag{2.2}$$

and the square of the strangeness radius,

$$r_s^2 = \int d^3r\langle p|\mathbf{r}^{\,2}\,\bar{s}\gamma_0 s|p\rangle. \tag{2.3}$$

In analogy to the electromagnetic case, the momentum dependence of the strangeness current matrix elements is contained in two form factors,

$$\langle p'|\bar{s}\gamma_\mu s|p\rangle = \overline{N}(p')\left(\gamma_\mu F_1^s(q^2) + i\frac{\sigma_{\mu\nu}q^\nu}{2M_N}F_2^s(q^2)\right)N(p), \tag{2.4}$$

where $q = p' - p$, and N is the free Dirac spinor of the nucleon. Strangeness conservation and the zero overall strangeness charge of the proton imply $F_1^s(0) = 0$.

It is often convenient to use the electric and magnetic form factors introduced by Sachs,

$$G_E^s(q^2) = F_1^s(q^2) + \frac{q^2}{4M_N^2}F_2^s(q^2),$$

$$G_M^s(q^2) = F_1^s(q^2) + F_2^s(q^2), \tag{2.5}$$

which describe the strangeness charge and current distribution, respectively. The above matrix elements for μ_s and r_s^2 are simply related to the form factors by

$$\mu_s = G_M^s(0), \qquad r_s^2 = 6\frac{d}{dq^2}G_E^s(q^2)|_{q^2=0}. \tag{2.6}$$

Note that we use the Sachs form factor, which corresponds to the physical charge distribution, to define the strangeness radius. An alternative definition, based on the Dirac form factor (i.e., F_1^s), has also been used in the literature.

For the following discussion it will be useful to recall the relation of the strangeness vector current to the other neutral vector currents and to the standard U(3) current nonet in the three-flavor sector,

$$J_\mu^a = \bar{q}\gamma_\mu \frac{\lambda^a}{2} q, \tag{2.7}$$

with $\lambda^0 \equiv \sqrt{2/3}$ and $\mathrm{tr}\{\lambda^a\lambda^b\} = 2\delta^{ab}$. In the standard flavor basis defined by Eq. (2.7), the neutral currents and the corresponding operators for the electric charge, the baryon number, and the hypercharge have the form

$$J_\mu^{\mathrm{el}} = \bar{q}\gamma_\mu Q^{\mathrm{el}} q = J_\mu^3 + \frac{1}{\sqrt{3}} J_\mu^8,$$

$$Q^{\mathrm{el}} = T^3 + \frac{Y}{2} = \frac{\lambda^3}{2} + \frac{\lambda^8}{2\sqrt{3}}, \tag{2.8}$$

$$J_\mu^B = \bar{q}\gamma_\mu B q = \frac{1}{\sqrt{6}} J_\mu^0, \quad B = \frac{1}{3}, \tag{2.9}$$

$$J_\mu^Y = \bar{q}\gamma_\mu Y q = \frac{2}{\sqrt{3}} J_\mu^8, \quad Y = B - S = \frac{\lambda^8}{\sqrt{3}}, \tag{2.10}$$

and the strangeness current can be written as

$$J_\mu^s = \bar{s}\gamma_\mu s = J_\mu^B - J_\mu^Y. \tag{2.11}$$

Note that we use the nonstandard sign convention of Jaffe [16] for the strangeness current. This leads to the negative sign of the strangeness contribution to the hypercharge in Eq. (2.10).

B. Experimental information

No direct measurement of the strange vector form factors has yet been performed. However, there is some (although indirect and rather uncertain) experimental evidence for them to be nonvanishing. A recent reanalysis [20] of the E734 experiment at BNL [5], which measured the elastic νp and $\bar{\nu}p$ differential cross sections in the momentum range $0.2\,\mathrm{GeV}^2 < Q^2 < 1.2\,\mathrm{GeV}^2$ to constrain the strange axial-vector form factor of the proton, indeed mildly favors nonzero vector form factors.

As suggested by Kaplan and Manohar [6], the authors of Ref. [20] refitted the E734 cross sections and, in contrast to the original analysis, allowed the strange vector form factors to be different from zero. Their analysis also takes the neutron electromagnetic form factor into account and fits the value of the mass parameter in the axial form factors, M_A. The observed elastic νp and $\bar{\nu}p$ scattering events and their statistical and systematical errors were binned in only seven Q^2 regions, which limits the number of fit parameters that can be determined from this data set. Garvey, Louis, and White [20] therefore determine only the lowest nonvanishing moments of the strange axial $[G^s(Q^2)]$ and vector $[F_1^s(Q^2), F_2^s(Q^2)]$ form factors, and assume the same momentum dependence as in the corresponding electromagnetic form factors.

Since no symmetry arguments connect the SU(3) singlet form factors with their octet counterparts, this is clearly a rather strong assumption. As we will discuss below, it is neither supported by the existing theoretical estimates nor by simple "quark-core plus meson-cloud" pictures of the nucleon. In the latter, one expects the electromagnetic charge and current distribution to be carried by a valence quark core and a meson cloud. Due to the absence of strange valence quarks one would expect a different, more outwards shifted strangeness distribution in this picture. We will discuss the dipole form further in the last section of this paper, where we compare it with our results and with another phenomenological estimate.

We do not, however, expect a different momentum dependence of F_1^s and F_2^s to change the fits of Ref. [20] significantly, since the neutrino cross sections are more sensitive to the strange axial form factor. The strong correlation between the fit values of $G^s(0)$ and M_A noted in Ref. [20] might, however, be enhanced by the assumed dipole form of G^s with $M_A^s = M_A$.

Although the existing data are not sufficient to strongly constrain any of the strange form factors, the difference in the Q^2 behavior of the neutrino— and antineutrino—proton cross sections seems to favor a finite, negative strangeness radius and a negative strangeness magnetic moment. As we will discuss in Sec. III C, these signs are expected if the nucleon's strangeness distribution arises mainly from fluctuations of its wave function into the hyperon plus kaon configuration.

Clearly, much more stringent experimental constraints on the strangeness form factors would be desirable. Some time ago, McKeown [21] and Beck [22] pointed out that neutral current form factors could be measured in parity-violating electron scattering experiments. Four such experiments are at present in different stages of preparation and will soon provide the first direct measurements of sea quark effects in low-energy observables. SAMPLE [12] at MIT-Bates plans to measure the value of F_2^s at $Q^2 = 0.1\,\mathrm{GeV}^2$ and will start to take data in less than a year. Three further experiments are located at CEBAF and will measure different combinations of the strange form factors in a larger range of momentum transfers. We refer the reader to Ref. [23] for a review of these experimental programs.

The sensitivity of this first generation of parity-violating elastic electron-proton scattering experiments will be high enough to distinguish among some of the present theoretical estimates of the strangeness radius and can therefore provide valuable and much needed constraints for nucleon models.

III. THE VECTOR STRANGENESS RADIUS AND MAGNETIC MOMENT

In this section we will discuss some of the theoretical estimates of the strangeness radius and magnetic moment. We will also add a new calculation of these quantities in models containing extended constituent quarks. The evaluation and discussion of the form factors for a larger momentum transfer region will be the subject of the subsequent section.

Let us point out from the beginning that all of the existing estimates are strongly model dependent and that none of them should be considered as a firm and reliable prediction. However, they give at least insight into the order of magnitude of the form factors and can thus provide motivation and guidance for future experiments. And, equally important, they explore and test different physical mechanisms for the appearance of a strangeness content in the nucleon.

A. The pole fit model

The first estimate of the strangeness radius and magnetic moment by Jaffe [16] is based on the pole fit of the isoscalar electromagnetic form factor of the nucleon of Höhler *et al.* [24], which assumes these form factors to be dominated by three (zero-width) isoscalar vector ($I^G J^{PC} = 0^-1^{--}$) meson states: the physical $\omega(780)$ and $\phi(1020)$ mesons and a third, higher-lying pole, which is intended to summarize the high-mass resonance and continuum contributions. (For a simpler estimate on the basis of a one-pole model and ω-ϕ mixing see Ref. [17].)

Adopting Höhler's three-pole ansatz also for the strangeness form factors, Jaffe writes F_1^s in the form of a once-subtracted dispersion relation [making use of $F_1^s(0) = 0$],

$$F_1^s(q^2) = \sum_{i=1}^{3} a_i^{(s)} \frac{q^2}{m_i^2 - q^2}, \tag{3.1}$$

whereas F_2^s is not normalized and taken unsubtracted,

$$F_2^s(q^2) = \sum_{i=1}^{3} b_i^{(s)} \frac{1}{m_i^2 - q^2}. \tag{3.2}$$

Höhler's form factors $F_{1,2}^{(I=0)}$ for the isoscalar part of the electromagnetic current (i.e., $J_\mu^{(I=0)} = \frac{1}{2} \cdot J_\mu^Y$) have exactly the same form. The corresponding masses m_i and coupling parameters $a_i^{(I=0)}, b_i^{(I=0)}$ have been determined by fits to the experimental data (see Table I).

Jaffe fixes all three masses in Eqs. (3.1) and (3.2)—including the one of the third pole—at the same values as in the isoscalar form factors of Ref. [24]; see Table I. The couplings $a_{1,2}^{(s)}$ and $b_{1,2}^{(s)}$ can be related to the corresponding couplings $a_{1,2}^{(I=0)}$ and $b_{1,2}^{(I=0)}$ by a simple quark counting prescription, starting from the flavor wave functions of the ω and ϕ mesons,

TABLE I. Fit parameters from Ref. [24]. $F_1^{I=0}(q^2) = \sum_i a_i/(m_i^2 - q^2)$, $F_2^{I=0}(q^2) = \sum_i b_i/(m_i^2 - q^2)$.

Fit number				
8.1	m_V (GeV)	0.78	1.02	1.40
	a_i (GeV)	0.71	-0.64	-0.13
	b_i (GeV)	-0.11	0.13	-0.02
8.2	m_V (GeV)	0.78	1.02	1.80
	a_i (GeV)	0.69	-0.54	-0.21
	b_i (GeV)	-0.14	0.20	-0.07
7.1	m_V (GeV)	0.78	1.02	1.67
	a_i (GeV)	0.68	-0.55	-0.24
	b_i (GeV)	-0.16	0.25	-0.08

$$|\omega\rangle = \cos\epsilon \frac{1}{\sqrt{2}} \left(|\bar{u}\gamma_\mu u\rangle + |\bar{d}\gamma_\mu d\rangle\right) - \sin\epsilon\, |\bar{s}\gamma_\mu s\rangle,$$

$$|\phi\rangle = \sin\epsilon\, |\omega_0\rangle + \cos\epsilon\, |\phi_0\rangle. \tag{3.3}$$

The small angle $\epsilon = 0.053$ [25] parametrizes the deviation from the ideally mixed states. The current-meson couplings are obtained from the assumption that a quark q_i with flavor i in the vector mesons couples only to the current $\bar{q}_i\gamma_\mu q_i$ of the same flavor, and with flavor-independent strength κ:

$$g(\omega, J^{I=0}) = \frac{\kappa}{\sqrt{6}} \sin(\theta_0 + \epsilon),$$

$$g(\phi, J^{I=0}) = -\frac{\kappa}{\sqrt{6}} \cos(\theta_0 + \epsilon),$$

$$g(\omega, J^s) = -\kappa \sin\epsilon,$$

$$g(\phi, J^s) = \kappa \cos\epsilon, \tag{3.4}$$

where θ_0 is the "magic angle" with $\sin^2\theta_0 = 1/3$. The vector-meson nucleon couplings are parametrized as $g_i(\omega_0, N) = g_i \cos\eta_i$, $g_i(\phi_0, N) = g_i \sin\eta_i$, where $i = 1, 2$ denotes the γ_μ and $\sigma_{\mu\nu}q^\nu$ couplings.

Comparing the above parametrization of the couplings with Höhler's fitted values for $a_{1,2}^{(I=0)}$ and $b_{1,2}^{(I=0)}$ leads to phenomenological values for the η_i and κg_i. The strangeness current couplings $a_{1,2}^{(s)}$ and $b_{1,2}^{(s)}$ are then obtained by simply replacing $J^{I=0}$ with J^s. The remaining couplings $a_3^{(s)}$ and $b_3^{(s)}$ are determined by imposing the (rather mild) asymptotic constraints $\lim_{q^2\to\infty} F_1^s(q^2) \to 0$, $\lim_{q^2\to\infty} q^2 F_2^s(q^2) \to 0$.

The strangeness radius and magnetic moment can now be obtained from Eqs. (2.5) and (2.6). Taking the average of the three fits in Ref. [24], Jaffe finds $r_s^2 = (0.14 \pm 0.07)\,\mathrm{fm}^2$ and $\mu_s = -(0.31 \pm 0.09)$. Note that these estimates are rather large—of the order of the corresponding electromagnetic moments of the neutron—and that they do not rely on a specific nucleon model. However, bias is introduced through the assumed three-pole ansatz for the form factors and the identification of the two light

poles with the physical ω and ϕ mesons. Furthermore, the final form of the ansatz relies on the conditions for the asymptotic behavior and on the parametrization of the couplings (which works well in the electromagnetic case).

As pointed out by Jaffe, the pole fit results depend crucially on Höhler's identification of the second pole with the physical ϕ meson, with its large strange quark content and its surprisingly strong, OZI-violating [49] coupling to the nucleon [26]. It should further be noted that adopting the third pole mass from Höhler *et al.* is hard to justify. The third pole does not correspond to a well-defined state, but rather summarizes unknown higher-lying resonance and continuum contributions, which will likely have a different distribution of strength for the hypercharge and strange currents.

Let us finally mention that the sign of r_s^2 is opposite to the one suggested by the reanalysis of the BNL neutrino scattering data of Garvey, Louis, and White, and found in other models, and that the three-pole ansatz does not allow the form factors to decay with the large powers of q^2 established via quark counting rules.

B. Skyrme model estimate

The first nucleon model estimate of the low-momentum strangeness form factors was based on the Skyrme model [17]. The latter is a topological soliton model, built on a chiral meson Lagrangian. Many variants of this model and of its treatment exist and are described, e.g., in the reviews [27]. The extension to the SU(3) flavor sector and its breaking is not unique and allows an even wider choice in the specific approach, which of course leads to some ambiguity in the results.

The authors of Ref. [17] choose the original Skyrme model [28] and introduce flavor symmetry breaking by nonminimal derivative terms in the Lagrangian. After canonical quantization in the restricted Hilbert space of collective and radial excitations, the Hamilton operator is diagonalized by treating the symmetry breaking terms exactly [29]. This approach in some sense combines the two conventional quantization schemes of the SU(3) skyrmion. From the strange vector form factors Ref. [17] obtains $r_s^2 = -0.10\,\mathrm{fm}^2$ and $\mu_s = -0.13$. In an extended Skyrme model containing vector mesons, these values drop by about a factor of two in magnitude, and the sign of the strangeness radius changes [30].

It is interesting that these results for nucleon sea quark distributions come from a model that describes quark physics rather indirectly in terms of meson fields. However, considerable theoretical uncertainties are associated with the Skyrme model estimates of the strange form factors. Besides the already-mentioned ambiguities in the specific choice of Lagrangian and SU(3) extension, there are several additional problems.

One serious concern is that the calculation of strange matrix elements in Skyrme-like models ultimately involves the small difference of two large but uncertain quantities, and hence is intrinsically unreliable. The source of this difficulty is that the strange vector current, which in QCD is understood at the quark level, must be described in terms of the Noether and topological currents in the Skyrme picture.

The strange current, in particular, is obtained from the relation of baryon number and hypercharge currents, Eq. (2.11):

$$J_\mu^s = J_\mu^B - J_\mu^Y \,. \tag{3.5}$$

Thus, r_s^2 is given by $r_B^2 - r_Y^2$. However, both r_B^2 and r_Y^2 are of order 1 fm^2 so that their difference is almost an order of magnitude smaller than the two separately. The above-mentioned problem arises, since quantities calculated in the Skyrme model have a typical accuracy at the 30% level (without introducing large numbers of parameters), which might even be expected from a model justified to leading order in a $1/N_c$ expansion, with $N_c = 3$.

Therefore, one concludes that the Skyrme model cannot accurately determine the strangeness radius to within several hundred percent, unless there are special reasons to believe that the errors in r_B^2 and r_Y^2 are strongly correlated. However, it is hard to argue for correlations in the errors, since they come from very different parts of the model. The baryon current is of topological origin, and it is difficult to understand why it should "know" about errors in the hypercharge current, which is a Noether current.

There is also a more fundamental concern with the Skyrme model calculation. The Skyrme model, and the approximations used to treat it, are generally believed to be justified in the large-N_c limit of QCD; effects of subleading contributions in $1/N_c$ are probably not reliable. This casts serious doubts on whether the Skyrme model (or any other large-N_c model) can ever make contact with strange matrix elements. After all, in a conventional treatment of the nucleon any strange quark matrix element must be ascribed to a Zweig-rule-violating amplitude. But, as argued by Witten [31] many years ago, Zweig's rule is exact in the large-N_c limit.

Apart from the question of whether the Skyrme model can give reliable strange quark matrix elements in light of the need for Zweig rule violations, there seems to be a paradox, since the approach of Ref. [17] continues to give nonzero strange matrix elements even as the parameters are pushed towards their $N_c \to \infty$ values. How can the model give *any* nonzero strange matrix element in the limit as $N_c \to \infty$?

The resolution of this "paradox" is simple: Since the nucleon is defined to be a member of the lowest $\mathrm{SU(3)_{flavor}}$ octet with N_c being any multiple of three, there are necessarily valence strange quarks in the nucleon for $N_c > 3$. To make a flavor octet out of N_c quarks, one groups the quarks in triples of flavor singlets except for the last three, which are coupled to an octet. The key point is that each of these groups of three quarks in a singlet state contains one strange quark. Thus, a nucleon with $N_c > 3$ will contain $\frac{N_c}{3} - 1$ valence strange quarks. A consequence of this fact is that the standard relation (3.5) between hypercharge, baryon number and strangeness must be modified for $N_c \neq 3$:

$$J^s_\mu = \frac{N_c}{3} J^B_\mu - J^Y_\mu \,. \tag{3.6}$$

Given the net strangeness content of nucleons in the large N_c world, there is no need for Zweig-rule-violating amplitudes. Indeed, as $N_c \to \infty$ the number of valence strange quarks diverges: The nucleon becomes infinitely strange. This fact explains why the Skyrme model can have nonzero strangeness matrix elements as $N_c \to \infty$.

The resolution of this paradox does not, however, affect the general conclusion that the ability of the Skyrme model to describe strange-quark matrix elements in the nucleon is likely to be fundamentally limited, due to its large N_c character. To describe our $N_c = 3$ world in the Skyrme model, one must start at the $N_c \to \infty$ world and attempt to extrapolate back, with inherent uncertainities in the $1/N_c$ correction terms. This procedure may be quite sensible for some quantities, if the underlying physics is essentially similar in the $N_c = 3$ and large N_c worlds. It is likely to be problematic for strange-quark matrix elements, however, since the character of the physics completely changes as N_c goes from infinity down to three. At large N_c there are a large number of valence strange quarks, and Zweig's rule is exact, while at $N_c = 3$ there are no valence strange quarks, and the entire contribution is due to Zweig rule violations.

C. The kaon-cloud model

In order to complement the pole and Skyrme model calculations, Musolf and Burkardt [18] estimated the strange vector matrix elements in yet another way, by considering the contributions arising from a K–Λ loop. The heavier K–Σ intermediate states have not been taken into account. As pointed out in Ref. [18], the corresponding couplings might, however, be significantly enhanced beyond their SU(3) values, which could make this contribution relevant.

In contrast to earlier attempts [32], the calculation of Ref. [18] uses the phenomenological meson-baryon form factors of the Bonn potential [33] to cut off the loop momentum and maintains gauge invariance via additional "seagull" vertices. The latter are generated from the Bonn form factors by the minimal-substitution prescription. (For an alternative choice of these form factors see Ref. [34].) The interaction of the strange vector current with the hadrons in the loop is treated as pointlike.

The above model is very likely to be too simple to provide quantitative predictions, since, e.g., contributions from other but the lightest hadrons are not taken into account. However, the motivation of the authors of Ref. [18] was not so much to end up with quantitative predictions, but rather to explore and discuss qualitative features of loop contributions.

The strange magnetic moment obtained in this approach lies in the range $\mu_s = -(0.31 - 0.40)$, dependent on the loop cutoff value, and is of about the same magnitude as the pole and Skyrme model predictions. The Sachs strangeness radius $r_s^2 = -(0.027 - 0.032)\,\mathrm{fm}^2$, however, has the sign opposite to the pole prediction, and its magnitude is smaller by a factor of 3 to 5.

In the chiral limit, the strangeness radius develops an infrared divergence from the meson propagator in the loop integral. It is therefore very sensitive to the meson mass if the latter becomes small. The Sachs radius, for example, would be an order of magnitude larger if the pion would replace the kaon in the loop, as it does in meson cloud models for the isovector part of the electromagnetic form factors. The SU(3) breaking effects are less pronounced for the magnetic moment, where the corresponding loop integrals are infrared finite.

Finally, in the absence of an agreement under the current theoretical estimates for the sign of the strangeness radius, another feature of the kaon cloud picture should be stressed: it provides a simple and intuitive argument for the origin of the sign of r_s^2. Since the (in our convention) negative strangeness charge in the loop is carried by the kaon, which is less than half as heavy as the lambda and thus reaches out further from the common center of mass, it contributes dominantly to r_s^2 and determines its negative sign.

This reasoning is analogous to the standard explanation for the negative sign of the electromagnetic charge radius of the neutron due to the negatively charged pion cloud. However, this static picture is, of course, oversimplified and neglects, in particular, recoil effects. The relevance of the latter can be seen in the dependence of the strangeness radii on the involved mass scales. The Dirac strangeness charge radius, for example, becomes positive for pointlike kaons (i.e., for large values of the cutoff mass in the meson-baryon form factors), whereas it stays negative if the kaon mass is replaced by the pion mass [18].

D. Kaon cloud and vector meson dominance

In this section we review our model for the strangeness form factors introduced in Ref. [19]. It combines an intrinsic form factor, taken for definiteness from the kaon cloud model discussed above, with vector meson dominance (VMD) [35] contributions and ω-ϕ mixing. We are focusing in the present section on the basic ideas underlying this approach and will give more details, together with the calculation of the full form factors, in Sec. IV.

The VMD hypothesis can, in its most general form, be summarized in terms of current field identities (CFI's) [36], which state the proportionality of the electromagnetic current and the field operators of light, neutral vector mesons with the same quantum numbers. The isocalar CFI has thus the general form

$$J^{(I=0)}_\mu = A_\omega\, m_\omega^2\, \omega_\mu + A_\phi\, m_\phi^2\, \phi_\mu, \tag{3.7}$$

with the couplings A_ω,A_ϕ yet to be fixed. Generalizing the VMD hypothesis to the strangeness current, we write an analogous CFI for J^s:

$$J^s_\mu = B_\omega\, m_\omega^2\, \omega_\mu + B_\phi\, m_\phi^2\, \phi_\mu. \tag{3.8}$$

It is convenient to combine these two CFI's into a vector

equation, so that the couplings form the elements of a matrix

$$\hat{C}_{I=0,s} = \begin{pmatrix} A_\omega & A_\phi \\ B_\omega & B_\phi \end{pmatrix}. \tag{3.9}$$

In order to fix the couplings in Eq. (3.9), we sandwich the CFI's between the physical vector meson states and the vacuum to obtain the following representation for $\hat{C}$:

$$\begin{pmatrix} \langle 0 | J_\mu^{(I=0)} | \omega \rangle & \langle 0 | J_\mu^{(I=0)} | \phi \rangle \\ \langle 0 | J_\mu^{s} | \omega \rangle & \langle 0 | J_\mu^{s} | \phi \rangle \end{pmatrix}$$

$$= \varepsilon_\mu \hat{C}_{I=0,s} \begin{pmatrix} m_\omega^2 & 0 \\ 0 & m_\phi^2 \end{pmatrix} \tag{3.10}$$

(ε_μ describes the polarization state of the vector mesons). We now determine the matrix elements on the left-hand side of Eq. (3.10) from the simple U(3) flavor counting rule discussed in Sec. III A. It states that the matrix element of the quark vector current of flavor i between the vacuum and the flavor-j component of the vector meson V (V stands for ω or ϕ) is diagonal in flavor and of universal strength κ, i.e.,

$$\langle 0 | \bar{q}_i \gamma_\mu q_i | (\bar{q}_j q_j)_V \rangle = \kappa m_V^2 \delta_{ij} \varepsilon_\mu. \tag{3.11}$$

With the flavor wave functions of ω and ϕ from Sec. III A and the currents $J_\mu^{I=0} = \frac{1}{2} J_\mu^Y$ and J_μ^s given in Eqs. (2.10) and (2.11) we then obtain

$$\hat{C}_{I=0,s}(\epsilon) = \kappa \begin{pmatrix} \frac{1}{\sqrt{6}} \sin(\theta_0 + \epsilon) & \frac{-1}{\sqrt{6}} \cos(\theta_0 + \epsilon) \\ -\sin\epsilon & \cos\epsilon \end{pmatrix}. \tag{3.12}$$

The same prescription for the couplings was used in Jaffe's pole fit; see Sec. III A. Both the magic angle $\theta_0 = \tan^{-1}(1/\sqrt{2})$ and the mixing angle ϵ, which relates the ideally mixed flavor states of the vector mesons to their physical states and is small and positive [37], have been introduced in Sec. III A. In the following, we will use $\epsilon = 0.053$, which has been determined in Ref. [25] from the $\phi \to \pi + \gamma$ decay width and is consistent with the decay width of $\phi \to \pi^+ + \pi^- + \pi^0$. Despite the small value of ϵ, the vector meson mixing will generate the dominant part of our result for the strangeness radius [19], which consequently acquires a rather strong ϵ dependence.

The CFI's lead to a general expression for the form factors. To derive it, we first note that Eqs. (3.7) and (3.8), together with the requirement of strangeness and hypercharge conservation, imply $\partial^\mu V_\mu = 0$ (V_μ stands for either ω_μ or ϕ_μ), which simplifies the field equations to

$$(\Box + m_V^2) V_\mu = J_\mu^{(V)} \tag{3.13}$$

and therefore also implies that the vector meson source currents are conserved ($\partial^\mu J_\mu^{(V)} = 0$). We now take nucleon matrix elements of the field equations (3.13) and use the CFI's to write

$$\begin{pmatrix} \langle N(p') | J_\mu^{(I=0)} | N(p) \rangle \\ \langle N(p') | J_\mu^{s} | N(p) \rangle \end{pmatrix} = \hat{C}_{I=0,s}(\epsilon) \begin{pmatrix} \frac{m_\omega^2}{m_\omega^2 - q^2} & 0 \\ 0 & \frac{m_\phi^2}{m_\phi^2 - q^2} \end{pmatrix} \begin{pmatrix} \langle N(p') | J_\mu^{(\omega)} | N(p) \rangle \\ \langle N(p') | J_\mu^{(\phi)} | N(p) \rangle \end{pmatrix}. \tag{3.14}$$

It is convenient to reexpress the vector meson source currents in terms of currents with the same SU(3) transformation behavior as $J^{(I=0)}$ and J^s, which we will denote as *intrinsic* ($J_{\rm in}$). The corresponding transformation can be written as

$$\begin{pmatrix} J_\mu^{(\omega)} \\ J_\mu^{(\phi)} \end{pmatrix} = \hat{D}_{I=0,s} \begin{pmatrix} J_{{\rm in},\mu}^{(I=0)} \\ J_{{\rm in},\mu}^{(s)} \end{pmatrix}. \tag{3.15}$$

Applying it on the right-hand side of Eq. (3.14) and separating the nucleon matrix elements into form factors, according to Eq. (2.4) and its analog for $J_\mu^{(I=0)}$, we obtain our general VMD expression for the form factors:

$$\begin{pmatrix} F^{I=0}(q^2) \\ F^s(q^2) \end{pmatrix} = \hat{C}_{I=0,s}(\epsilon) \begin{pmatrix} \frac{m_\omega^2}{m_\omega^2 - q^2} & 0 \\ 0 & \frac{m_\phi^2}{m_\phi^2 - q^2} \end{pmatrix} \hat{C}_{I=0,s}^{-1}(\epsilon) \begin{pmatrix} F_{\rm in}^{I=0}(q^2) \\ F_{\rm in}^{s}(q^2) \end{pmatrix}. \tag{3.16}$$

According to their definition, the intrinsic form factors describe the extended source current distribution of the nucleon to which the vector mesons couple. Since both $J^{(I=0)}$, $J^{(s)}$ and their intrinsic counterparts $J_{\rm in}^{(I=0)}$, $J_{\rm in}^{(s)}$ are conserved, the full and the intrinsic form factors in Eq. (3.16) have the same normalization at $q^2 = 0$. This immediately implies $\hat{D}_{I=0,s} = \hat{C}_{I=0,s}^{-1}$ and has been anticipated in writing Eq. (3.16). Combining Eqs. (3.16) and (3.12), we finally obtain

$$\begin{pmatrix} F^{I=0}(q^2) \\ F^s(q^2) \end{pmatrix} = \begin{pmatrix} \frac{m_\omega^2}{m_\omega^2 - q^2} \frac{\sin(\theta_0+\epsilon)\cos\epsilon}{\sin\theta_0} - \frac{m_\phi^2}{m_\phi^2 - q^2} \frac{\cos(\theta_0+\epsilon)\sin\epsilon}{\sin\theta_0} & \frac{\cos(\theta_0+\epsilon)\sin(\theta_0+\epsilon)}{\sqrt{6}\sin\theta_0} \left(\frac{m_\omega^2}{m_\omega^2 - q^2} - \frac{m_\phi^2}{m_\phi^2 - q^2} \right) \\ \frac{\sqrt{6}\cos\epsilon\sin\epsilon}{\sin\theta_0} \left(\frac{m_\phi^2}{m_\phi^2 - q^2} - \frac{m_\omega^2}{m_\omega^2 - q^2} \right) & \frac{m_\phi^2}{m_\phi^2 - q^2} \frac{\cos\epsilon\sin(\theta_0+\epsilon)}{\sin\theta_0} - \frac{m_\omega^2}{m_\omega^2 - q^2} \frac{\sin\epsilon\cos(\theta_0+\epsilon)}{\sin\theta_0} \end{pmatrix}$$

$$\times \begin{pmatrix} F_{\rm in}^{I=0}(q^2) \\ F_{\rm in}^{s}(q^2) \end{pmatrix}. \tag{3.17}$$

A couple of instructive features can be directly read off from this expression. First, the dependence on both the vector-meson-current and vector-meson-nucleon couplings has dropped out. This is a straightforward consequence of charge normalization, which requires both couplings to cancel each other, and is a general feature of VMD form factors [35]. As a consequence we have $F(0) = F_{\rm in}(0)$ for both the strangeness and the isoscalar form factor. Note that the normalization of the intrinsic isoscalar form factor $[F_{1,\rm in}^{I=0}(0) = 1/2]$ differs from that in Ref. [19], where we used a different isoscalar current. The strangeness radius and magnetic moment remain the same, however.

Up to now our discussion has been rather general, and different choices for the intrinsic form factors can be implemented in this framework. A very important restriction on every such choice is, however, that it does not lead to double counting with the physics of the VMD sector. We will come back to this issue later.

In order to calculate the strangeness form factor from Eq. (3.17) explicitly, we have to specify the intrinsic form factors. As in Ref. [19], we adopt the kaon loop model from the last section [18] for the intrinsic strangeness form factor but use the physical value for the Λ mass (Ref. [18] takes the flavor-symmetric value, i.e., the nucleon mass). One could think of adopting an analogous pion cloud model for the intrinsic isoscalar electromagnetic form factor. Since, however, typical models for intrinsic nucleon charge distributions require a large quark core contribution in addition to the pion cloud [38], we do not expect intrinsic electromagnetic form factors to be sufficiently well modeled by pion loops, and we will therefore follow a different strategy.

We first adopt Höhler's fit [24] of the isoscalar form factor to the experimental data, summarized for convenience in Table I. From this fit we extract the *intrinsic* isoscalar form factor by inverting the VMD matrix in Eq. (3.17). Then we determine the strangeness form factor from the second row of Eq. (3.17). The contribution from the intrinsic strangeness part to the isoscalar form factor is very small and plays almost no role in the determination of $F_{\rm in}^{I=0}(q^2)$.

Since the strangeness magnetic moment is obtained from the magnetic form factor at $q^2 = 0$, it is not modified by the vector mesons and originates solely from the intrinsic contribution. It has therefore the same value as in the kaon loop model. Both the Dirac and the Sachs strangeness radii, however, get an additive contribution from the vector mesons. This contribution increases the charge radius by about a factor of 3, $r_{s,\rm Dirac}^2 = -(0.0243 - 0.0245)\,\mathrm{fm}^2$, and the Sachs radius by about a factor of 2, $r_s^2 = -(0.040 - 0.045)\,\mathrm{fm}^2$. Both signs are the same as those of the intrinsic contribution.

This enhancement in the strangeness radii is rather important from the perspective of experiments. The charge radius obtained from the kaon cloud alone is too small, for example, to be detected in the planned parity-violating elastic ep scattering experiments, whereas the enhancement due to the vector mesons could lead to an observable effect.

A couple of other aspects of the VMD approach should be noted. The VMD part of the form factors is generic and independent of any details of the model except the general VMD form. In particular, it is independent of the current-meson couplings with their underlying theoretical assumptions and uncertainties. It also renders the strangeness radius less sensitive to the model dependence of the intrinsic form factors. The kaon cloud form factors alone are, for example, dominated by the strongly parametrization-dependent seagull contributions.

Another important aspect of the VMD results is their crucial dependence on the ω–ϕ mixing. Indeed, the strangeness radius would not receive any contribution from ideally mixed vector meson states, since the nucleon has no overall intrinsic strangeness. As a consequence, the VMD contribution to the radius is proportional to the sine of the mixing angle ϵ.

E. Constituent quark models

In this section we will discuss the strangeness radius from the point of view of a large class of hadron models based on a constituent quark core. In the "naive" nonrelativistic constituent quark models, the quarks are pointlike and, since sea quarks are absent, there is no mechanism for a nonvanishing strangeness distribution in the nucleon. However, it was argued some time ago [6] that the constituent quark picture can be generalized to accommodate a finite strangeness content. Indeed, if one regards a constituent quark as a QCD current quark surrounded by a complicated, nonperturbative cloud of gluons and $q\bar{q}$ pairs, then even up and down constituent quarks can have a strangeness distribution.

Of course, predictions of the nucleon's strangeness distribution in such constituent quark models have still to relate the strangeness content of the constituent quark to that of the nucleon. This is no simple task and generally requires the solution of a relativistic Fadeev-type equation.[2]

Fortunately, however, the nucleon's strangeness Sachs radius can be inferred exactly from that of the constituent quark without any specific calculation, and it is independent of the interquark dynamics. To see this, consider a system of three constituent quarks with strange charge distributions $\rho_s(\mathbf{r}-\mathbf{r}_i)$ of identical shape, centered at (in general, time-dependent) positions $\mathbf{r}_i$. The total strangeness radius of the nucleon is then

$$r_s^2 = \int dV\, \mathbf{r}^2\, [\rho_s(\mathbf{r}-\mathbf{r}_1) + \rho_s(\mathbf{r}-\mathbf{r}_2) + \rho_s(\mathbf{r}-\mathbf{r}_3)]\,, \tag{3.18}$$

[2]First studies of this type in the Nambu–Jona-Lasinio (NJL) model have recently reproduced the nucleon mass quite well [39], but they are not easily generalizable to the calculation of form factors. Furthermore, it is not obvious that they are consistent with the Hartree-Fock or large-N_c approximations used to derive the constituent quark propagators.

and after shifting the integration variable by the individual positions of the quarks one obtains

$$r_s^2 = 3\int dV\,\mathbf{r}^2\rho_s(\mathbf{r}) + 2(\mathbf{r}_1+\mathbf{r}_2+\mathbf{r}_3)\cdot\int dV\,\mathbf{r}\,\rho_s(\mathbf{r}) + (\mathbf{r}_1^2+\mathbf{r}_2^2+\mathbf{r}_3^2)\int dV\,\rho_s(\mathbf{r}) = 3\,(r_s^2)_q. \quad (3.19)$$

The last equation holds for isotropic quark strangeness distributions with vanishing overall strangeness charge and shows that the nucleon strangeness radius is, under the stated conditions, just the sum of the quark strangeness radii.[3]

The above ideas can be studied quantitatively in models which generate constituent quarks dynamically by dressing the elementary quarks with $q\bar{q}$ pairs. The prototype of this class of models has been introduced by Nambu and Jona-Lasinio (NJL) [40], and the first study of the scalar strangeness content of constituent quarks in this framework can be found in Ref. [41].

In order to give an estimate of the nucleon strangeness radius in constituent quark models, all that remains to be done is to calculate the strangeness radius of the constituent quark itself. We will perform such a calculation in the remainder of this section in the context of the NJL model. An extensive study of electromagnetic quark and meson properties in different SU(3) generalizations of the NJL model can be found in Refs. [42,43], and we will employ some of their results.

A strangeness component in the valence constituent quarks can only be generated by OZI-rule-violating processes, which require a flavor-mixing interaction. In the conventional Hartree-Fock approximation to the NJL model (on which the work of Ref. [43] is based), flavor mixing originates exclusively from determinantal six-quark interactions [41]. These terms, of the form of 't Hooft's instanton-generated effective Lagrangian [44], represent the anomalous breaking of the $U(1)_A$ symmetry in QCD, and contain two coupling constants, H and H'. Their physical role is primarily to generate the mass splittings of the singlet and octet states in the pseudoscalar channel (H) and of the ρ and ω mesons in the vector channel (H'). In addition, these couplings will determine the strangeness content of the constituent quark.

We start our calculation by writing the constituent U quark matrix elements of the strangeness current as

$$\langle U(p')|J_\mu^s(0)|U(p)\rangle = \overline{U}(p')\left(\gamma_\mu f_1^s(q^2) + i\frac{\sigma_{\mu\nu}q^\nu}{2m_u}f_2^s(q^2)\right)U(p) = \sum_\nu [\mathcal{F}(q^2)]_{\mu,\nu}^{s,u}\overline{U}(p')\Gamma^\nu U(p). \quad (3.20)$$

[3]Note that the isotropy condition could be violated by the strangeness current (as opposed to charge) distribution, which prevents us from extending the above argument to the strange magnetic moment. Note also that two- or three-body correlations between the quarks, beyond or instead of the common mean-field potential, could invalidate the isotropy condition.

The form factor matrix $\mathcal{F}$ is, in Hartree-Fock approximation, a solution of the Bethe-Salpeter-type equation

$$\mathcal{F} = 1 + \mathcal{K}\mathcal{J}\mathcal{F}\,, \quad (3.21)$$

where $\mathcal{K}$ is the effective two-body reduction of the NJL interaction, containing the coupling constants, and $\mathcal{J}$ is the so-called generating correlation function, which is basically a two-body propagator. The explicit forms of both $\mathcal{K}$ and $\mathcal{J}$ are given in Ref. [42].

The Sachs strangeness radius of the constituent u quark,

$$(r_s^2)_u = 6\left.\frac{dg_E^s(q^2)}{dq^2}\right|_{q^2=0}\,, \quad (3.22)$$

can now be obtained from the explicit solutions for f_1^s and f_2^s, given in [43], and $g_E^s = f_1^s + (q^2/4m_u^2)f_2^s$. We find

$$(r_s^2)_u = \frac{96\sqrt{2}H'\langle\bar{u}u\rangle}{D^{I=0}(0)}m_u m_s I_s\left(-2G_2 I_u + \frac{1}{4m_u^2}\right)\,, \quad (3.23)$$

where

$$D^{I=0}(0) = 1 - 8m_u^2 H'\langle\bar{s}s\rangle I_u - 128m_u^2 m_s^2 (H'\langle\bar{u}u\rangle)^2 I_u I_s \quad (3.24)$$

and the integrals I_q can be solved analytically:

$$I_q = \frac{3}{4\pi^2}\left[\frac{\Lambda^2}{\Lambda^2+m_q^2} + \ln\left(\frac{m_q^2}{\Lambda^2+m_q^2}\right)\right]\,. \quad (3.25)$$

With the parameters of Ref. [42], $m_u = m_d = 364\,\mathrm{MeV}$, $m_s = 522\,\mathrm{MeV}$, $\Lambda = 0.9\,\mathrm{GeV}$, $G_2\Lambda^2 = 2.51$, and $H'\Lambda^2\langle\bar{s}s\rangle = -4.4\times10^{-2}$, we finally obtain the numerical value

$$r_s^2 = 3\,(r_s^2)_u = 1.69\times10^{-2}\,\mathrm{fm}^2. \quad (3.26)$$

It comes somewhat as a surprise that r_s^2 has the opposite sign as the VMD result, since the isoscalar and isovector form factors of the NJL constituent quarks are also dominated by vector meson intermediate states [43]. However, Eq. (3.23) shows that the NJL result is proportional to H' (which sets the singlet-octet mass splitting in the vector sector), whereas ω-ϕ mixing, which gave rise to the VMD contribution to r_s^2, occurs also for $H' = 0$ (in the case of $m_u^0 \neq m_s^0$). This indicates that physics other than VMD contributes substantially to the NJL result. Note furthermore that the entire result depends on subleading effects in $1/N_c$ counting.

In Table II we summarize all the theoretical estimates of the nucleon strangeness radius discussed above.

IV. THE STRANGENESS FORM FACTORS

Our discussion has so far mainly focused on the first nonvanishing moments of the nucleon strangeness dis-

TABLE II. Theoretical results for the strange magnetic moment and strangeness radius.

Source	μ_s (μ_N)	r_s^2 (fm^2)	Ref.
Poles	-0.31±0.09	0.14 ± 0.07	[16]
Kaon loops [SU(3) symm.]	- (0.31 – 0.40)	- (2.71 – 3.23)×10^{-2}	[18]
Kaon-loops	- (0.24 – 0.32)	-(2.23 – 2.76)×10^{-2}	[19]
VMD	- (0.24 – 0.32)	-(3.99 – 4.51)×10^{-2}	[19]
NJL		1.69×10^{-2}	This work
SU(3) Skyrme	-0.13	-0.11	[17]

tribution. These quantities—the strangeness radius and magnetic moment—will be the first characteristics of the strange form factors to be measured, and thus have received most of the theoretical attention.

However, not only does the higher momentum region of the form factors contain important physical information, but its knowledge is also required for the interpretation of the currently prepared experiments to measure r_s^2 and μ_s (and the already discussed BNL neutrino scattering experiment). Since the form factors cannot be measured exactly at $q^2 = 0$, the data have to be extrapolated back to the light point from small spacelike q^2. The extracted values for r_s^2 and μ_s will thus depend on the assumed momentum dependence of the form factors, and its better understanding is clearly important.

In the absence of reliable information, one sometimes parametrizes the momentum dependence, as in the electromagnetic form factors, in Galster's dipole form. This choice is motivated by simplicity and convenience, but has no theoretical basis. The physics contributing to the strange form factors—originating exclusively from sea quarks—might well lead to a momentum dependence other than the dipole form (which also does not reproduce the asymptotic behavior suggested by quark counting rules). Note, however, that a Galster form with independent mass parameters to be determined by experiment, as proposed in Ref. [45], could be sufficiently flexible to describe the form factors in the momentum range relevant for CEBAF.

In the present section we will extend our work on the simple VMD plus kaon cloud model (proposed in Ref. [19] and discussed in the last section) to the calculation of the strangeness vector form factors in the momentum region accessible at CEBAF. Since our approach is based on low-energy dynamics, however, it will not be applicable at larger q^2.

The momentum dependence of the VMD contribution was already given in Eq. (3.17). The intrinsic form factors will be determined in the kaon cloud model of Ref. [18]. Even if the corresponding kaon loop graphs to be calculated are UV finite, the effective hadronic description of the underlying physics breaks down at large momenta. We will therefore follow Ref. [18] and attach form factors,

$$H(k^2) = \frac{m_K^2 - \Lambda^2}{k^2 - \Lambda^2} , \tag{4.1}$$

taken from the Bonn potential [46], to the meson-nucleon vertices to cut off the loop momenta. The Bonn values for the cutoff Λ in the $N\Lambda K$ vertex were extracted from fits to baryon-baryon scattering data and lie in the range of 1.2–1.4 GeV.

As already mentioned, the J_μ^s-hadron couplings will be assumed pointlike and therefore given by the strangeness charge of the struck hadron. Also, in order to maintain gauge invariance in the presence of the extended meson-baryon vertices, we have to introduce seagull vertices. These vertices are generated from the effective Lagrangian

$$\mathcal{L}_{N\Lambda K} = -ig_{N\Lambda K}\bar{\Psi}\gamma_5\Psi H(-\partial^2)\phi , \tag{4.2}$$

where Ψ and ϕ represent baryon and kaon fields, by minimal substitution in the gradient operator. This prescription [47], while not unique, generates the seagull vertex

$$i\Gamma_\mu(k,q) = \mp g_{N\Lambda K}Q_K\gamma_5(q \pm 2k)_\mu \times \frac{H(k^2) - H((q \pm k)^2)}{(q \pm k)^2 - k^2} , \tag{4.3}$$

where Q_K is the kaon strangeness charge, and the upper (lower) sign corresponds to an incoming (outgoing) meson. As expected, this vertex disappears in the limit $\Lambda \to \infty$ of pointlike couplings.

We can now identify three distinct contributions to the intrinsic form factors. The three corresponding amplitudes are associated with processes in which the current couples either to the baryon line (B), the meson line (M), or the meson-baryon vertex (V) in the loop, and are given by

$$\Gamma_\mu^B(p',p) = -ig_{N\Lambda K}^2 Q_\Lambda \int \frac{d^4k}{(2\pi)^4}\Delta(k^2)H(k^2)\gamma_5 S(p'-k)\gamma_\mu S(p-k)\gamma_5 H(k^2) , \tag{4.4}$$

$$\Gamma_\mu^M(p',p) = -ig_{N\Lambda K}^2 Q_K \int \frac{d^4k}{(2\pi)^4}\Delta((k+q)^2)(2k+q)_\mu\Delta(k^2)H((k+q)^2)\gamma_5 S(p-k)\gamma_5 H(k^2) , \tag{4.5}$$

$$\Gamma^V_\mu(p',p) = -ig^2_{N\Lambda K}Q_K \int \frac{d^4k}{(2\pi)^4} H(k^2)\Delta(k^2)\left[\frac{(q+2k)_\mu}{(q+k)^2-k^2}[H(k^2) - H((k+q)^2)]\right.$$
$$\left. \times\gamma_5 S(p-k)\gamma_5 - \frac{(q-2k)_\mu}{(q-k)^2-k^2}[H(k^2) - H((k-q)^2)]\gamma_5 S(p'-k)\gamma_5\right]. \quad (4.6)$$

$\Delta(k^2) = (k^2 - m_K^2 + i\epsilon)^{-1}$ is the kaon propagator, $S(p-k) = (\not{p} - \not{k} - M_\Lambda + i\epsilon)^{-1}$ is the Λ propagator, $p' = p + q$ with q being the photon momentum, and Q_Λ is the Λ strangeness charge. In our convention (where the s quark has strangeness $+1$) $Q_\Lambda = 1$ and $Q_K = -1$. The values of the coupling and masses used are $M_N = 939\,\mathrm{MeV}$, $M_\Lambda = 1116\,\mathrm{MeV}$, $m_K = 496\,\mathrm{MeV}$ and $g_{N\Lambda K}/\sqrt{4\pi} = -3.944$ [46]. It is easy to show that these three amplitudes satisfy the Ward-Takahashi identity.

The intrinsic strangeness form factors are obtained by writing the nucleon matrix element of the sum of these amplitudes in terms of Dirac and Pauli form factors

$$\overline{N}(p')\Gamma_\mu(p',p)N(p) = \overline{N}(p')\left(\gamma_\mu F^s_{1,\mathrm{in}}(q^2) + i\frac{\sigma_{\mu\nu}q^\nu}{2M_N}F^s_{2,\mathrm{in}}(q^2)\right)N(p)\,, \quad (4.7)$$

where N is the nucleon spinor. The corresponding electric and magnetic Sachs form factors can be obtained from Eq. (2.5).

The dependence of the electric strangeness form factor on the (spacelike) momentum transfer $Q^2 = -q^2$ is shown as the full line in Fig. 1 and, for comparison, the result of the pole fit model [16] is also plotted. The results are quite different both in size and magnitude, and document the present state of theoretical uncertainty. We further plot the intrinsic contribution alone, which essentially corresponds to the full form factor in the model of Ref. [18]. While it has the same sign as our result and is of comparable magnitude, its slope at the origin, and consequently the mean square strangeness radius, is by a factor of 3 smaller.

It is interesting to see how much of the form factor in our approach comes from the VMD contribution alone, i.e., by treating the core as pointlike and by setting $F^{I=0}_{1,\mathrm{in}}(Q^2) = 1/2$ and $F^s_{1,\mathrm{in}}(Q^2) = 0$. While the slope at the origin is slightly reduced in this case, the overall behavior of the form factor remains almost unchanged.

In Fig. 2 we show the dependence of G^s_E on the parameters of the intrinsic form factors. While Höhler's three different fits for the intrinsic isoscalar form factor $F^{I=0}_{\mathrm{in}}$ have almost no influence on our result and cannot be distinguished in Fig. 2, we see a mild dependence on the kaon loop cutoff in the range between $\Lambda = 1.2\,\mathrm{GeV}$ and $\Lambda = 1.4\,\mathrm{GeV}$, which is compatible with the Bonn potential fits. We also plot the pole fit result [16] for the three fits (fit Nos. 7.1, 8.1, and 8.2) of the isoscalar form factor and find a rather strong dependence.

Figure 3 shows the magnetic strangeness form factor in our model and again, for comparison, the pole fit result. As in the case of the electric form factor, their slopes at the origin, their curvatures and their momentum dependence are generally rather different. However, the values at $Q^2 = 0$, i.e., the strange magnetic moments, are quite similar. Since the VMD contribution does not alter the value of μ_s, given by $G^s_{M,\mathrm{in}}(0)$, the intrinsic form factor

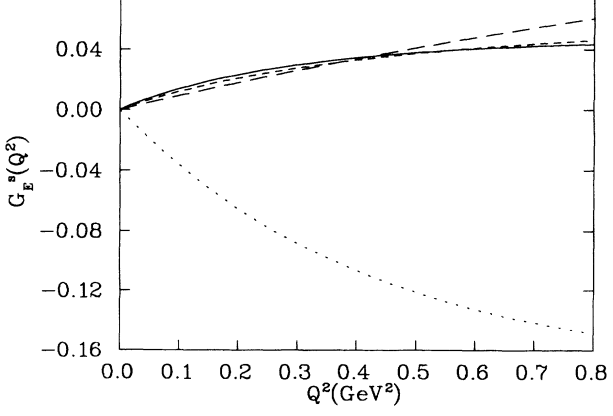

FIG. 1. The Q^2 dependence of the electric strangeness form factor using $\Lambda = 1.2\,\mathrm{GeV}$. The solid line represents our result. The long-dashed line gives the intrinsic contribution, and the short-dashed line gives only the VMD contribution. The dotted line is the result of Ref. [16] with the fit 8.1 of Table I.

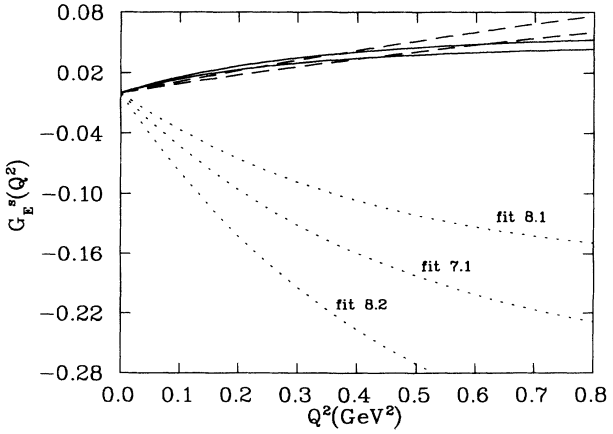

FIG. 2. Same as Fig. 1 but for two values of Λ. The upper solid and long-dashed lines are for $\Lambda = 1.4\,\mathrm{GeV}$, and the lower solid and long-dashed lines are for $\Lambda = 1.2\,\mathrm{GeV}$. The dotted lines are the results of Ref. [16] for the three different fits in Table I.

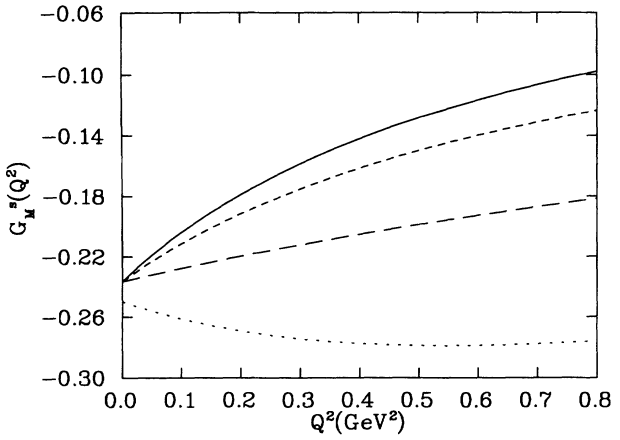

FIG. 3. The Q^2 dependence of the magnetic strangeness form factor using $\Lambda = 1.2\,\mathrm{GeV}$. The solid line represents our result. The long-dashed line gives the intrinsic contribution, and the short-dashed line gives only the VMD contribution. The dotted line is the result of Ref. [16] with the fit 8.1 of Table I.

starts at the same value as the full G_M^s but is, in contrast to G_E^s, considerably smaller. The VMD contribution alone, however, is not as close to the complete result as in the case of G_E^s. (To generate this graph we kept the intrinsic isoscalar and strange form factors constant, at their values at $Q^2 = 0$.)

The $G0$ experiment at CEBAF [13] will measure the Q^2 dependence of G_M^s in the momentum range $0.1\,\mathrm{GeV}^2 < Q^2 < 0.5\,\mathrm{GeV}^2$, with a resolution $\delta\mu_s \simeq \pm 0.22$ at low Q^2, and decreasing for larger Q^2. The SAMPLE experiment at MIT-Bates [12] will determine μ_s with comparable experimental error, and the combined data might thus be sufficient to distinguish between our and the pole result.

The dependence of G_M^s on the cutoff and on the choice of fit for $F_{\mathrm{in}}^{I=0}$ can be seen in Fig. 4. While our result is still practically insensitive to the choice of fit, the variation with the kaon loop cutoff, again in the range $\Lambda = (1.2 - 1.4)\,\mathrm{GeV}$, is stronger than for the electric form factor. The dependence of the pole fit result on the choice of fit is even larger, as for G_E^s.

We have already mentioned that some authors, and in particular Garvey, Louis, and White in their reanalysis of the BNL neutrino scattering experiment [20], used a Galster dipole parametrization

$$F_1^s(Q^2) = \frac{F_1^s Q^2}{\left(1 + \frac{Q^2}{4M_N^2}\right)\left(1 + \frac{Q^2}{M_V^2}\right)^2}, \tag{4.8}$$

$$F_2^s(Q^2) = \frac{F_2^s(0)}{\left(1 + \frac{Q^2}{M_V^2}\right)^2}, \tag{4.9}$$

for the Q^2 dependence of the strange form factors, in which $M_V = 0.843\,\mathrm{GeV}$ is taken to be the same as in the electromagnetic form factors. As mentioned before, a more general form of the Galster parametrization, in which the masses are taken as independent fit parameters, has been proposed in Ref. [45]. The reanalysis of the E734 experiment gave a first idea of the leading momentum dependence, $F_2^s(0) = -0.40 \pm 0.72$ and $F_1^s = -(1/6)(r_s^2)_{\mathrm{Dirac}} = (0.53 \pm 0.70)\,\mathrm{GeV}^2$, although these values have large error bars and are consistent with zero. Furthermore, the assumptions that had to be made for the neutron form factors add to the theoretical uncertainties of this reanalysis.

Still, the estimates of Ref. [20] allow us to assess the compatibility of the dipole form with our results and those of the pole fit. In Figs. 5 and 6 we compare our Dirac and Pauli form factors and those of Ref. [16] with the dipole forms, Eqs.(4.8) and (4.9). The differences between the three approaches are clearly more pronounced for F_1^s. Figure 5 also indicates that the value for the Dirac strangeness radius, if extracted by fitting the momentum dependence of the dipole parametrization, can be rather different from the one obtained in other estimates. The

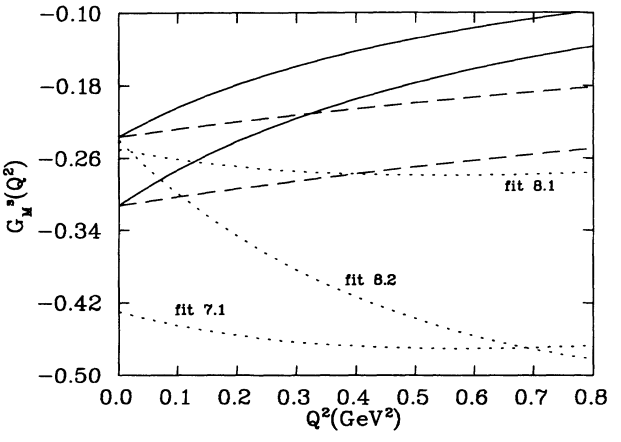

FIG. 4. Same as Fig. 3 but for two values of Λ. The upper solid and long-dashed lines are for $\Lambda = 1.2\,\mathrm{GeV}$ and the lower solid and long-dashed lines are for $\Lambda = 1.4\,\mathrm{GeV}$. The dotted lines are the results of Ref. [16] for the three different fits in Table I.

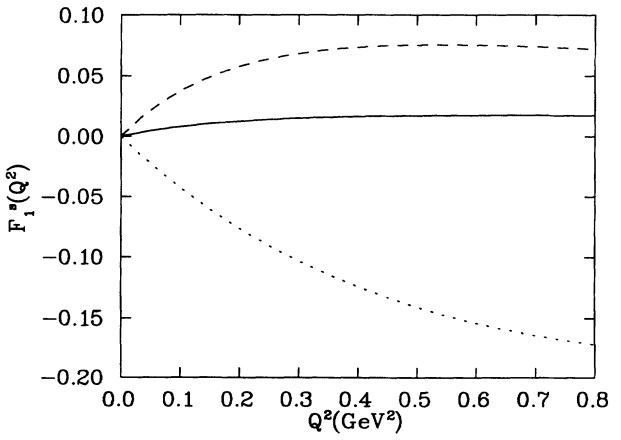

FIG. 5. The Q^2 dependence of the Dirac strangeness form factor using $\Lambda = 1.2\,\mathrm{GeV}$. The solid line represents our result. The dashed and dotted lines are the results of Refs. [20] and [16], respectively.

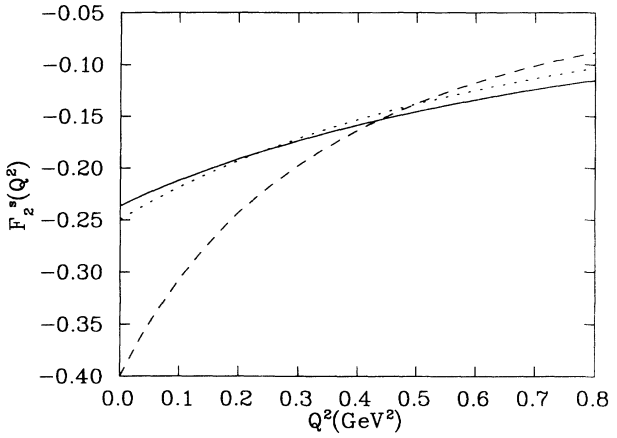

FIG. 6. Same as Fig. 5 for the Pauli strangeness form factor. Note the similarity of all three predictions at intermediate momentum transfers.

same holds for the strange magnetic moment, as can be seen in Fig. 6. On the other hand, all three results for $F_2^s(Q^2)$ (Fig. 6) look rather similar in the momentum region $0.4\,\mathrm{GeV}^2 < Q^2 < 0.8\,\mathrm{GeV}^2$, in which the data will be taken at CEBAF.

Finally, comparing our approach to some of the other proposed mechanisms, we note interesting differences in the role played by vector meson mixing. Whereas the rather small deviation of the ω and ϕ states from ideal mixing is indispensable for a nonvanishing VMD contribution to the strangeness radius in our approach, this is not so in the pole fit model of Ref. [16].

Indeed, in the pole model r_s^2 gets bigger as the mixing angle ϵ goes to zero. In our approach, on the other hand, the Dirac form factor reduces in the same limit to

$$F^s(q^2) = \frac{m_\phi^2}{m_\phi^2 - q^2} F_{\mathrm{in}}^s(q^2)\,, \tag{4.10}$$

and the strangeness current interacts with the nucleon only through the ϕ meson. In particular, the strangeness radius does not get any contribution from VMD in the limit of ideal mixing, since the nucleon has no intrinsic strangeness [i.e., $F_{\mathrm{in}}^s(0) = 0$].

V. SUMMARY AND CONCLUSIONS

In this paper we present a theoretical estimate for the strangeness vector form factors of the nucleon in the momentum region relevant for the planned experiments at MIT-Bates and CEBAF. This estimate is based on our previously introduced model of the nucleon strangeness distribution in terms of a kaon cloud, a vector meson dominance contribution and ω-ϕ mixing.

We find both Sachs form factors to be dominated by the VMD contribution. The electric strangeness form factor, in particular, is left practically unchanged if the intrinsic contribution is taken pointlike. For the same reason, the dependence of our result on the meson-baryon form factor masses in the kaon loops is very weak. Both the sign and the slope of the electric form factor are opposite to those of the pole fit estimate. Together with the considerably larger slope of the pole fit result at zero momentum transfer, this leads already at moderate momentum transfer to a significant difference in magnitude between the two form factors.

Although the intrinsic kaon cloud contribution plays a somewhat more important role in the magnetic Sachs form factor, its overall shape and slope are again mainly determined by the vector mesons. The value at zero momentum transfer, i.e., the strangeness magnetic moment, however, is not modified by the VMD contribution and thus shows a more pronounced dependence on the intrinsic meson-baryon form factors. As in the case of the electric form factor, the overall qualitative behavior of our result, and, in particular, its slope and curvature, differs considerably from the pole fit estimate.

We also compare our results to a Galster dipole parametrization, with the cutoff masses fixed at the same values as in the electromagnetic form factors, which has been used to reanalyze the BNL E734 neutrino scattering experiment. The Dirac dipole form factor has the same sign and curvature as ours, but with a considerably larger overall size and slope at the origin, whereas the Pauli form factors agree rather closely for the momenta to be probed at CEBAF, i.e., for $Q^2 > 0.4\,\mathrm{GeV}^2$.

Since our results, with the exception of the strange magnetic moment, are dominated by the vector meson sector, they show a largely reduced sensitivity to the rather strong model dependence of the intrinsic contribution. The intrinsic form factors from the kaon cloud model adopted in this paper, for example, receive their main contribution from the seagull vertices, which are determined by a minimal, but not unique prescription.

The vector meson dominance mechanism, on the other hand, has a robust and largely generic character. It introduces no free parameters and does not leave much freedom in its implementation. In particular, however, it is based on phenomenologically successful physics, which is well established from the electromagnetic interactions of hadrons.

We further study the nucleon strangeness radius from the point of view of a class of constituent quark models in which the constituent quarks have an extended structure. The valence up and down quarks in the nucleon can then acquire an intrinsic strangeness distribution. We point out that the strangeness radius of the nucleon is model independently given by the sum of the constituent quark radii, since their strangeness charge distribution is isotropic and since their overall strangeness is zero. For a quantitative estimate we employ the Nambu–Jona-Lasinio model and find a 2–3 times smaller value than in the kaon-loop-VMD model with the opposite sign.

In order to put these results into perspective, we also review and discuss some of the other existing theoretical estimates. Comparing the results for the strangeness radius and magnetic moment reveals in particular the large discrepancies between those predictions. Both signs of the strangeness radius, for example, and values within a range of an order of magnitude have been found. Clearly the theoretical uncertainties are at present not reliably

under control and the existing results have to be regarded as order-of-magnitude estimates.

This situation reflects both the size of the challenge with which the nonvalence strangeness sector confronts existing hadron models, and our present lack of insight from the first principles of QCD. While first attempts to study the effects of disconnected quark loops on the lattice have been reported [48], it will still take considerable time and effort before reliable results for the strange quark content of the nucleon can be expected. In the meantime, however, the data from Bates and CEBAF will constrain the existing hadron models and test their underlying physics. It thus seems guaranteed that the subject will remain intriguing and challenging in the years to come.

ACKNOWLEDGMENTS

T.D.C., H.F., and X.J. acknowledge support from the U.S. Department of Energy under Grant No. DE–FG02–93ER–40762. T.D.C. and X.J. acknowledge additional support from the National Science Foundation under Grant No. PHY–9058487. M.N. acknowledges the warm hospitality and congenial atmosphere provided by the University of Maryland Nuclear Theory Group and support from FAPESP Brazil.

[1] A. DeRujula, H. Georgi, and S.L. Glashow, Phys. Rev. D **12**, 147 (1975); N. Isgur and G. Karl, *ibid.* **18**, 4187 (1978).
[2] J. Ashman *et al.*, Phys. Lett. B **206**, 364 (1988).
[3] J. Ashman *et al.*, Nucl. Phys. **B328**, 1 (1989).
[4] J. Ellis and R.L. Jaffe, Phys. Rev. D **9**, 1444 (1974); R.L. Jaffe and A. Manohar, Nucl. Phys. **B337**, 509 (1990).
[5] L.A. Ahrens *et al.*, Phys. Rev. D **35**, 785 (1987).
[6] D.B. Kaplan and A. Manohar, Nucl. Phys. **B310**, 527 (1988).
[7] T.P. Cheng, Phys. Rev. D **13**, 2161 (1976).
[8] T.P. Cheng and R. Dashen, Phys. Rev. Lett. **26**, 594 (1971).
[9] J.F. Donoghue and C.R. Nappi, Phys. Lett. B **168**, 105 (1986).
[10] J. Gasser, H. Leutwyler, and M.E. Sainio, Phys. Lett. B **253**, 252 (1991).
[11] See, for example, J.P. Blaizot, M. Rho, and N. Scoccola, Phys. Lett. B **209**, 27 (1988).
[12] MIT/Bates Proposal No. 89-06, R. McKeon and D.H. Beck, contact people.
[13] CEBAF Proposal No. PR-91-017, D.H. Beck, spokesperson.
[14] CEBAF Proposal No. PR-91-004, E.J. Beise, spokesperson.
[15] CEBAF Proposal No. PR-91-010, J.M. Finn and P.A. Souder, spokespeople.
[16] R.L. Jaffe, Phys. Lett. B **229**, 275 (1989).
[17] N.W. Park, J. Schechter, and H. Weigel, Phys. Rev. D **43**, 869 (1991).
[18] M.J. Musolf and M. Burkardt, Z. Phys. C **61**, 433 (1994).
[19] T.D. Cohen, H. Forkel, and M. Nielsen, Phys. Lett. B **316**, 1 (1993).
[20] G.T. Garvey, W.C. Louis, and D.H. White, Phys. Rev. C **48**, 761 (1993).
[21] R.D. McKeown, Phys. Lett. B **219**, 140 (1989).
[22] D.H. Beck, Phys. Rev. D **39**, 3248 (1989).
[23] M.J. Musolf, T.W. Donnelly, J. Dubach, S.J. Pollock, S. Kowalski, and E.J. Beise, Phys. Rep. **239**, 1 (1994).
[24] G. Höhler *et al.*, Nucl. Phys. **B114**, 505 (1976).
[25] P. Jain *et al.*, Phys. Rev. D **37**, 3252 (1988).
[26] H. Genz and G. Höhler, Phys. Lett. B **61**, 389 (1976).
[27] I. Zahed and G.E. Brown, Phys. Rep. **142**, 1 (1986); U.-G. Meissner, *ibid.* **161**, 213 (1988).
[28] T.H.R. Skyrme, Proc. R. Soc. London, Ser. A **247**, 260 (1958), **262**, 236 (1959).
[29] H. Yabu and K. Ando, Nucl. Phys. B **301**, 601 (1988).
[30] N.W. Park and H. Weigel, Nucl. Phys. A **541**, 453 (1992).
[31] E. Witten, Nucl. Phys. B **160**, 57 (1979).
[32] B.R. Holstein, in *Proceedings of the Caltech Workshop on Parity Violation in Electron Scattering, Pasadena, 1989*, edited by E.J. Beise and R.D. McKeown (World Scientific, Singapore, 1990), pp. 27–43; W. Koepf, E.M. Henley, and S.J. Pollock, Phys. Lett. B **288**, 11 (1992).
[33] R. Machleidt, in *Advances in Nuclear Physics*, edited by J.W. Negele and E. Vogt (Plenum, New York, 1989), Vol. 19, p. 189.
[34] W. Koepf and E.M. Henley, Phys. Rev. C **49**, 2219 (1994).
[35] J.J. Sakurai, *Currents and Mesons* (University of Chicago Press, Chicago, 1969); R.K. Bhaduri, *Models of Nucleon*, Lecture Notes and Supplements in Physics No. 22 (Addison-Wesley, New York, 1988), Chap. 7.
[36] N.M. Kroll, T.D. Lee, and B. Zumino, Phys. Rev. **157**, 1376 (1967).
[37] Particle Data Group, Phys. Rev. D **45**, 1 (1992).
[38] G.E. Brown and M. Rho, Comments Nucl. Part. Phys. **15**, 245 (1986); **18**, 1 (1988).
[39] N. Ishii, W. Bentz, and K. Yazaki, Phys. Lett. B **301**, 165 (1993); S.-Z. Huang and J. Tjon, Phys. Rev. C **49**, 1702 (1994).
[40] Y. Nambu and G. Jona-Lasinio, Phys. Rev. **124**, 246, 255 (1961).
[41] V. Bernard, R.L. Jaffe, and U.-G. Meissner, Nucl. Phys. B **308**, 753 (1988).
[42] S. Klimt, M. Lutz, U. Vogl, and W. Weise, Nucl. Phys. A **516**, 429 (1990).
[43] U. Vogl, M. Lutz, S. Klimt, and W. Weise, Nucl. Phys. A **516**, 469 (1990).
[44] G. 't Hooft, Phys. Rev. Lett. **37**, 8 (1976); Phys. Rev. D **14**, 3432 (1976).
[45] M.J. Musolf and T.W. Donelly, Nucl. Phys. A **546**, 509 (1992).
[46] B. Holzenkamp, K. Holinde, and J. Speth, Nucl. Phys. A **500**, 485 (1989).
[47] K. Ohta, Phys. Rev. D **35**, 785 (1987).
[48] S.J. Dong and K.F. Liu, Phys. Lett. B **328**, 130 (1994).
[49] S. Okubo, Phys. Lett. **5**, 165 (1963); G. Zweig, CERN Report No. TH 412, 1964 (unpublished); I. Iizuka, Prog. Theor. Phys. Suppl. **37–38**, 21 (1966).